REFERENCES

[1] R. P. Owens, J. E. Aitken, and T. C. Edwards, "Quasi-static characteristics of microstrip on an anisotropic sapphire substrate," *IEEE Trans. Microwave Theory Tech.*, vol. MTT-24, pp. 499–505, Aug. 1976.

[2] B. T. Szentkuti, "Simple analysis of anisotropic microstrip lines by a transform method," *Electron. Lett.*, vol. 12, pp. 672–673, Dec. 1976.

[3] M. Kobayashi and R. Terakado, "Accurately approximate formula for the effective filling fraction for microstrip lines with isotropic substrates and its application to the case with anisotropic substrate," *IEEE Trans. Microwave Theory Tech.*, vol. MTT-27, pp. 776–778, Sept. 1979.

[4] M. Horno, "Quasi-static characteristics of microstrip on arbitrary anisotropic substrates," *Proc. IEEE*, vol. 86, pp. 1033–1034, Aug. 1980.

[5] N. G. Alexopoulos, S. Kerner, and C. M. Krowne, "Dispersionless coupled microstrip over fused silica-like anisotropic substrate," *Electron. Lett.*, vol. 12, pp. 579–580, Oct. 1976.

[6] M. Kobayashi, "Analysis of the microstrip and the electrooptic light modulator," *IEEE Trans. Microwave Theory Tech.*, vol. MTT-26, pp. 119–126, Feb. 1978.

[7] M. Kobayashi and R. Terakado, "Method for equalizing phase velocities of coupled microstrip lines by using anisotropic substrates," *IEEE Trans. Microwave Theory Tech.*, vol. MTT-28, pp. 719–722, July 1980.

[8] M. Horno, "Upper and lower bounds on capacitances of coupled microstrip lines with anisotropic substrates," *Proc. Inst. Elec. Eng.*, vol. 129, pt. H, no. 3, pp. 89–93, June 1982.

[9] N. G. Alexopoulos and S. G. Maas, "Characteristics of microstrip directional couplers on anisotropic substrates," *IEEE Trans. Microwave Theory Tech.*, vol. MTT-30, pp. 1267–1270, Aug. 1982.

[10] M. Horno, "Quasistatic characteristics of covered coupled microstrip on anisotropic substrates: Spectral and variational analysis," *IEEE Trans. Microwave Theory Tech.*, vol. MTT-30, pp. 1888–1892, Nov. 1982.

[11] N. G. Alexopoulos and S. G. Maas, "Performance of microstrip couplers on an anisotropic substrate with an isotropic superstrate," *IEEE Trans. Microwave Theory Tech.*, vol. MTT-31, pp. 671–672, Aug. 1983.

[12] M. Horno, F. Medina, and R. Marqués, "Quasistatic characteristics of shielded coupled microstrip lines on anisotropic substrates," in *Proc. of II Int. IEEE Mediterranean Electrotech. Conf. (MELECON'83)*, (Athens, Greece), May 1983, pp. B5.05.

[13] S. K. Koul and B. Bath, "Generalized analysis of microstrip-like transmission lines and coplanar strips with anisotropic substrates for MIC, electrooptic modulator, and SAW applications," *IEEE Trans. Microwave Theory Tech.*, vol. MTT-31, pp. 1051–1059, Dec. 1983.

[14] T. Kitazawa and Y. Hayashi, "Coupled slot on an anisotropic sapphire substrate," *IEEE Trans. Microwave Theory Tech.*, vol. MTT-29, pp. 1035–1040, Oct. 1981.

[15] T. Kitazawa and Y. Hayashi, "Quasistatic characteristics of coplanar waveguides on a sapphire substrate with optical axes inclined," *IEEE Trans. Microwave Theory Tech.*, vol. MTT-30, pp. 920–922, June 1982.

[16] W. R. Smythe, *Static and Dynamic Electricity*. New York: McGraw Hill, 1968, ch. 3, pp. 54.

[17] M. Horno and R. Marqués, "Coupled microstrips on double anisotropic layers," *IEEE Trans. Microwave Theory Tech.*, vol. MTT-32, pp. 467–470, Apr. 1984.

Theoretical and Experimental Study of a Novel *H*-Guide Transverse Slot Antenna

M. KISLIUK, SENIOR MEMBER, IEEE, AND
A. AXELROD, STUDENT MEMBER, IEEE

Abstract—**Transverse slots in the "upper" plate of a dielectric-loaded parallel plane waveguide (*H*-guide) operating in the dominant mode (zero cutoff frequency) are proposed as slot antennas.**

A new theoretical approach to the analysis of a single-slot antenna is presented, leading to explicit expressions for the antenna input impedance and radiation efficiency. The computed values of the VSWR and radiation efficiency are in good agreement with laboratory measurements. The radiation efficiency of a single slot exceeds 10 percent in the 8–11-GHz frequency band, reaching a 50-percent theoretically predicted maximum at the slot resonance frequency, when the guide is terminated by a matched load.

Experimental checks prove that the leakage, or parasitic, radiation power level is less than −40 dB relative to the measured radiated power.

Manuscript received July 20, 1984; revised January 4, 1985.

The authors are with the Department of Electron Devices and Electromagnetic Radiation, Faculty of Engineering, Tel-Aviv University, Tel-Aviv 69978, Israel.

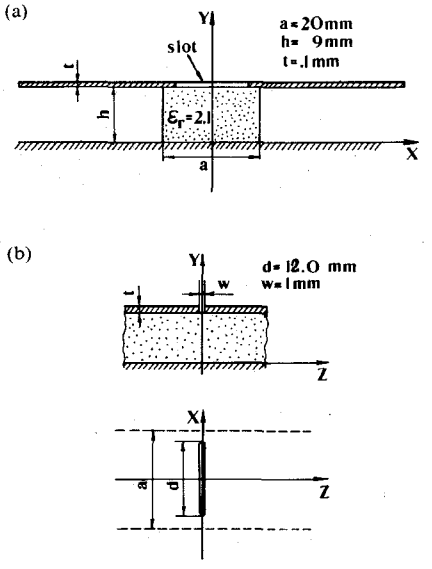

Fig. 1. (a) The *H*-guide cross section. (b) Geometry of the slot radiator.

I. INTRODUCTION

Microwave conformal antennas are widely used in many airborne and spaceborne systems. The conventionally used microstrip resonator antennas are mostly narrow band, have a poor radiation efficiency, and the parasitic radiation from the feeding microstriplines [1] interferes with the radiation from the resonator.

The *H*-guide proposed by F. J. Tisher [2], [3], or the parallel plane waveguide partially filled with a dielectric [4], can be fabricated as thin as a microstrip board, and successfully used for conformal mounting. M. Cohn showed [4] that "the dominant mode TE_{10}" of this guide (zero cutoff frequency) can be used for wide-band applications. The electric field of this mode is perpendicular to the metallic plates (Fig. 1), and neither the propagation constant, nor the wave impedance of this mode depend on the thickness of the guide. The fringe fields of the *H*-guide can be reduced to 60–80 dB by choosing the right width of the plates, thus excluding any leakage side radiation.

A theory of a single transverse, symmetrically spaced slot antenna (Fig. 1) is presented in Section II. Closed-form expressions for the normalized input impedance, the VSWR, and the radiation efficiency of a single-slot antenna are obtained. It is shown that 50 percent is the upper theoretical limit of the radiation efficiency of a single series slot radiator in any waveguide structure terminated by a matched load.

Laboratory measurements of the VSWR and radiation efficiency of a single slot (Figs. 5 and 6) are presented in Section III, and the measured values are in good agreement with the developed theory. The experiments confirm the theoretically predicted 50-percent radiation efficiency at VSWR = 3.0 of a single slot at resonance.

No significant change in the values of the reflected and transmitted waves has been detected when the measurements were repeated with metallic screens mounted across the side gaps of

0018-9480/85/0500-0428$01.00 ©1985 IEEE

the guide. These measurements proved the absence of any leakage side radiation; direct measurements performed during radiation pattern tests showed that the leakage radiation power level was less than -40 dB relative to the slot radiation.

II. Theory of a Transverse Slot Radiator

Consider a parallel plane waveguide partially filled with a dielectric (Fig. 1) supporting the dominant mode TE_{10} [4] (H-guide supporting the PE_{10} mode [5]).

A transverse slot is cut in the upper metallic plate of the guide. Following the classical theory of waveguide slot antennas [6], [7], there is an incident wave, traveling in the positive z-direction

$$\boldsymbol{E}_{\text{inc}} = \hat{y} C f(x) \exp(-j\beta_g z) \tag{1a}$$

$$\boldsymbol{H}_{\text{inc}} = -\hat{x}\frac{C}{Z_w} f(x) \exp(-j\beta_g z) + \hat{z} H_{z,\text{inc}} \tag{1b}$$

and two scattered waves. The reflected wave is

$$\boldsymbol{E}_r = \hat{y} B f(x) \exp(j\beta_g z) \tag{2a}$$

$$\boldsymbol{H}_r = \hat{x}\frac{B}{Z_w} f(x) \exp(j\beta_g z) + \hat{z} H_{z,r} \tag{2b}$$

and the electric field of the wave scattered in the forward direction is

$$\boldsymbol{E}_t = \hat{y} A f(x) \exp(-j\beta_g z). \tag{3}$$

The wave impedance and the propagation constant of the mode are

$$Z_w = \eta k/\beta_g \tag{4a}$$

$$\beta_g^2 = \epsilon_r k^2 - \xi^2 = k^2 + \alpha^2 \tag{4b}$$

$$\eta = \sqrt{\mu_0/\epsilon_0} \quad k = \omega\sqrt{\mu_0\epsilon_0}. \tag{4c}$$

The transverse wavenumber is calculated from the equation

$$\frac{\xi}{\cos(a\xi/2)} = k\sqrt{\epsilon_r - 1} \tag{5}$$

and $f(x)$ defines the distribution of the fields (1)–(3)

$$f(x) = \begin{cases} \cos(\xi x), & \text{for } |x| \leqslant a/2 \\ \cos(\xi a/2) \exp[-(|x| - a/2)\alpha], & \text{for } |x| \geqslant a/2 \end{cases} \tag{6}$$

The electric field on the slot is

$$\boldsymbol{E}_s = \hat{z} V_0 \frac{1}{w} \varphi(x), \qquad \varphi(0) = 1 \tag{7}$$

where $\varphi(x)$ is the voltage distribution on the slot.

As shown in [7], the amplitudes of the scattered waves (in a waveguide terminated by a matched load) are

$$B = -V_0 \frac{M_1}{2M_2} = -A \tag{8}$$

and the equivalent circuit of the slot is a series impedance, as shown in Fig. 2.

$$M_1 = \frac{1}{w}\int_{\text{slot}} \varphi(x) f(x) \exp(-j\beta_g z)\, dx\, dz \tag{9}$$

$$M_2 = 2h\int_0^\infty f^2(x)\, dx. \tag{10}$$

The voltages and the characteristic impedance of the guide (Fig. 2) are found from energy considerations [7], [8]

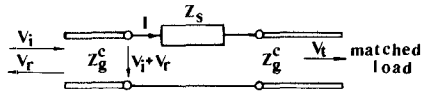

Fig. 2 Equivalent circuit of a narrow transverse slot in the upper plate of an H-guide.

$$V_i = hC \quad V_r = hB \quad V_t = (C - B)h \tag{11}$$

$$Z_g^c = Z_w \frac{h^2}{M_2}. \tag{12}$$

The complex power delivered to the impedance Z_s is

$$S_{\text{slot}} = \frac{|V_i + V_r - V_t|^2}{2Z_s} = 2\frac{|B|^2}{Z_s^*} h^2.$$

Hence, the normalized impedance of the slot is [8]

$$Z_{sn} = 2\frac{M_2|B|^2}{Z_w S_{\text{slot}}^*} \tag{13}$$

which is a generalization of the classical expression [7]; the asterisks denote complex conjugate values.

The complex power S_{slot} of the equivalent impedance Z_s (Fig. 2) accounts for the complex power radiated by the slot into free space, and for the reactive power of the evanescent modes generated by the slot inside the guide.

Any waveguide-fed narrow radiating slot is equivalent to a lossy slotline [9] short-circuited at both ends, and excited by a distributed current source $J_s(x)$. The length b of the equivalent line is somewhat greater than the physical slot length d (see Appendix). The voltage across the slot satisfies the transmission-line equation

$$\frac{d^2 V_s}{dx^2} - \gamma_s^2 V_s = -\gamma_s Z_c J_s(x) \tag{14a}$$

and the boundary conditions

$$V_s(\pm b/2) = 0 \tag{14b}$$

where

$$\gamma_s = \alpha_s + j\beta_s \tag{15}$$

and Z_c are, respectively, the complex propagation constant and the characteristic impedance of the slotline.

The linear density of the surface current $J_s(x)$ that excites the slot is

$$J_s(x) = \frac{1}{w}\int_{-w/2}^{w/2} (-\hat{z})\cdot \boldsymbol{K}(x,z)\, dz \tag{16}$$

where $\boldsymbol{K}$ is the surface current density equivalent to the x-component of the magnetic field on the aperture of the slot. From (1), it follows (if $d < a$) that

$$\boldsymbol{K}(x,z) = \hat{y} \times (-\hat{x})\, H_0 \cos(\xi x) \exp(-j\beta_g z) \tag{17}$$

which yields

$$J_s(x) = -H_0 \operatorname{sinc}(\beta_g w/2) \cos(\xi x) \tag{18}$$

where

$$\operatorname{sinc}(x) = \sin(x)/x. \tag{19}$$

The substitution of (18) into (14) yields the following solution [9] for the voltage distribution on the slot (7):

$$V_s(x) = V_0\varphi(x) \tag{20}$$

$$\varphi(x) = \frac{\cosh(\gamma_s b/2)\cos(\xi x) - \cos(\xi b/2)\cosh(\gamma_s x)}{\cosh(\gamma_s b/2) - \cos(\xi b/2)} \tag{21}$$

$$V_0 = -H_0 M_4 \tag{22}$$

$$M_4 = Z_c\gamma_s \frac{\cosh(\gamma_s b/2) - \cos(\xi b/2)}{(\xi^2 + \gamma_s^2)\cosh(\gamma_s b/2)} \operatorname{sinc}(\beta_g w/2). \tag{23}$$

The complex power consumed by the equivalent slotline is

$$S_{\text{slot}} = -\frac{1}{2}\int_{\text{slot}} \boldsymbol{E}_s \cdot \boldsymbol{K}^* \, dx\,dz$$

and after the substitution of (7), (17), and (22)

$$S_{\text{slot}} = \frac{|V_0|^2}{2}\frac{M_1}{M_4^*}. \tag{24}$$

From (13) and (24), it follows that the normalized impedance of the slot (Fig. 2) is

$$Z_{sn} = \frac{M_1 M_4}{Z_w M_2} \tag{25}$$

and the reflection coefficient of the slot in a waveguide terminated by a matched load is

$$\Gamma = \frac{Z_{sn}}{Z_{sn}+2}, \qquad \Gamma = B/C. \tag{26}$$

If the magnetic field H_0 in (17) is chosen as the sum of the incident (1) and reflected (2) waves

$$H_0 = (C - B)/Z_w \tag{27}$$

the substitution of (27) into (22) and (8) yields the same expressions for Γ and Z_{sn} as above. The integrals (9) and (10) permit one to obtain an explicit expression for Z_{sn}

$$Z_{sn} = \frac{Z_c\beta_g b^2}{2\eta kah}\operatorname{sinc}^2(\beta_g w/2)\, Q_1/Q_2 \tag{28a}$$

where

$$Q_1 = u(u^2+v^2)[1+\operatorname{sinc}(2v)] - 2u^2\tanh(u)\cos^2(v) - uv\sin(2v) \tag{28b}$$

$$Q_2 = (u^2+v^2)^2[1+\operatorname{sinc}(2va/b)] + 2\cos^2(va/b)/(\alpha a) \tag{28c}$$

$$u = \gamma_s b/2 \quad v = \xi b/2. \tag{28d}$$

Expressions (28) contain the characteristic impedance Z_c and the complex propagation constant (15) of a dielectric-backed radiating slot. The effective dielectric constant of this slot is assumed [10] to be

$$\epsilon_e = q(\epsilon_r + 1) \tag{29a}$$

where q is 0.5 in the case of zero metal plate thickness ($t = 0$). Therefore, the propagation constant is

$$\beta_s = k\sqrt{\epsilon_e} \tag{29b}$$

and the characteristic impedance is

$$Z_c = Z_a/\sqrt{\epsilon_e} \tag{29c}$$

where Z_a is the characteristic impedance of the same slot without the dielectric substrate.

Explicit expressions for Z_a of a center-fed radiating slot cut in an infinite conductive plane are derived in the Appendix. At the resonant frequency of the slot, Z_a is 430 Ω (for $d/w = 12$) and changes very little with frequency (±3 percent in a 40-percent frequency band).

The attenuation constant α_s, which accounts for radiation losses, is found in the following way. The average power radiated into free space by a dielectric-backed slot with a cosine voltage distribution is [8]

$$P_{\text{rad}} = |V_0|^2 T/(8\pi\eta) \tag{30a}$$

where V_0 is the voltage at the center of the slot, and

$$T = (n^2+1)(T_1 - T_2)/n \tag{30b}$$

$$n = \sqrt{\epsilon_e} \tag{30c}$$

$$T_1 = \operatorname{Cin}[\pi(1+1/n)] - \operatorname{Cin}[\pi(1-1/n)] - \frac{2n}{n^2+1}[1+\cos(\pi/n)] \tag{30d}$$

$$T_2 = \pi(n^2-1)\{\operatorname{Si}[\pi(1+1/n)] - \operatorname{Si}[\pi(1-1/n)]\}/(n^2+1) \tag{30e}$$

$$\operatorname{Si}(x) = \int_0^x \frac{\sin(t)}{t}\,dt \quad \operatorname{Cin}(x) = \int_0^x \frac{1-\cos(t)}{t}\,dt.$$

The power delivered to an equivalent center-fed lossy transmission line is (see Appendix)

$$P_{\text{rad}} = \frac{|V_0|^2}{Z_c}\tanh(\alpha_s b/2). \tag{31}$$

From (31) and (30a), it follows

$$\alpha_s = \frac{2}{b}\tanh^{-1}\left(\frac{TZ_c}{8\pi\eta}\right). \tag{32}$$

Expressions (29) and (32), and the values obtained in the Appendix for Z_a, supply all the required parameters for the computation of the equivalent normalized impedance of the slot (28), and the reflection coefficient (26).

The radiation efficiency of the slot, which is the ratio of the average power dissipated in Z_s to the power carried by the incident wave (Fig. 2), is

$$\epsilon = P_{\text{slot}}/P_{\text{inc}} \tag{33a}$$

$$P_{\text{slot}} = \operatorname{Re}(S_{\text{slot}}) \quad P_{\text{inc}} = M_2|C|^2/(2Z_w). \tag{33b}$$

The substitution of (13) yields

$$\epsilon = 4\operatorname{Re}(|\Gamma|^2/Z_{sn}^*)$$

and, from (26), it follows

$$\epsilon = 4\frac{R_{sn}}{(R_{sn}+2)^2 + X_{sn}^2}. \tag{34}$$

Straightforward differentiations show that the maximum value of the radiation efficiency, which is 50 percent, can be achieved only when the following two conditions are satisfied simultaneously:

$$X_{sn} = 0 \quad R_{sn} = 2 \tag{35}$$

which means $\Gamma = 0.5$ and VSWR = 3.0.

III. Experimental Study

The tested single-slot H-guide antenna (Fig. 1) was fed from a standard metallic waveguide. The transition from the metallic waveguide to the H-guide was performed by flaring the metallic

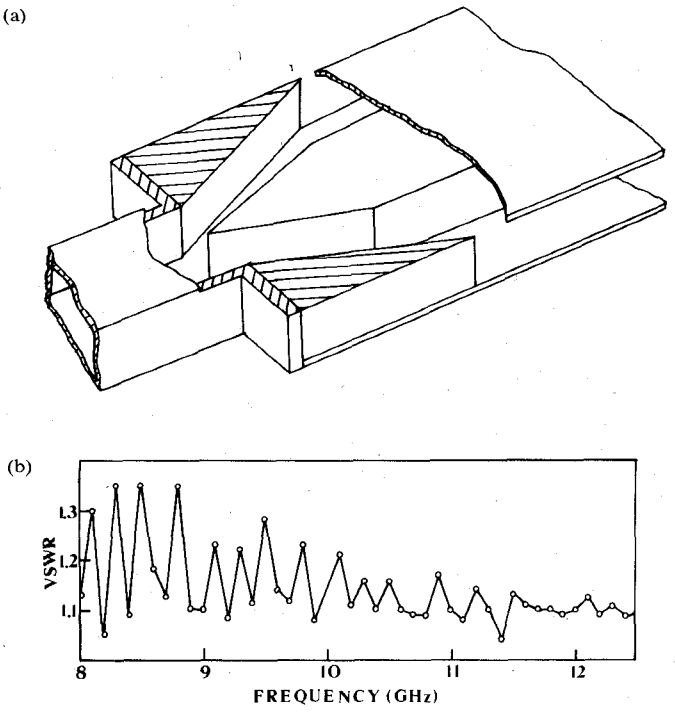

Fig. 3. (a) Transition from metallic waveguide to the H-guide. (b) The measured VSWR of a 60-cm-long section of H-guide with two transitions and dummy load at its far end.

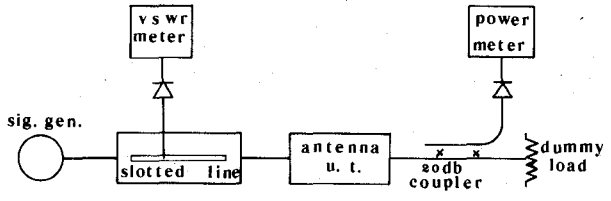

Fig. 4. The VSWR and radiation efficiency measurement setup.

guide in the H-plane, and tapering the dielectric slab of the H-guide, as shown in Fig. 3(a). The measured VSWR of a 60-cm-long section of an unslotted H-guide with two transitions and a dummy matched load at its end is plotted in Fig. 3(b).

The diagram of the experimental set for measuring the slot antenna VSWR and radiation efficiency is shown in Fig. 4. The reflection coefficients were measured with the slot open, and with the slot closed by a copper plate, and denoted, respectively, by Γ_0 and Γ_c. The respective levels of the power transmitted through the guide were P_0 and P_c, while the power of the incident wave P_{inc} was maintained at a constant level.

The radiation efficiency of the slot is

$$\epsilon = 1 - |\Gamma_0|^2 - P_i/P_{\text{inc}} - P_0/P_{\text{inc}} \tag{36a}$$

where P_i is the power dissipated due to intrinsic losses. The last term in (36a) can be represented as

$$P_0/P_{\text{inc}} = x\left(1 - |\Gamma_c|^2 - P_i/P_{\text{inc}}\right) \tag{36b}$$

where $x = P_0/P_c$. The substitution of (36b) into (36a) yields

$$\epsilon = 1 - |\Gamma_0|^2 - x + x|\Gamma_c|^2 + (x-1)P_i/P_{\text{inc}}. \tag{36c}$$

If the last small term in (36c) is neglected, the measured value of the radiation efficiency of the slot is

$$\epsilon = 1 - |\Gamma_0|^2 - x + x|\Gamma_c|^2. \tag{37}$$

The measured values of the VSWR and the radiation efficiency are presented in Figs. 5 and 6. The resonance of the slot occurs at

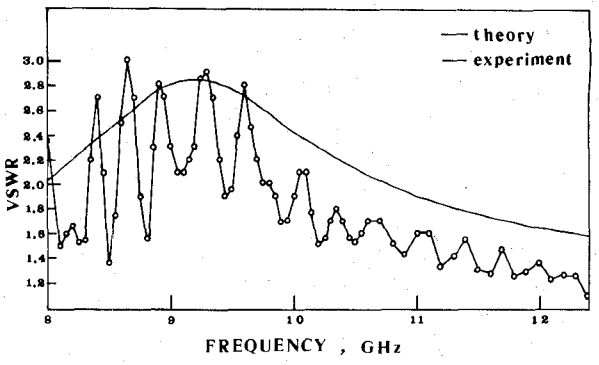

Fig. 5. The computed and measured VSWR of a single-slot radiator.

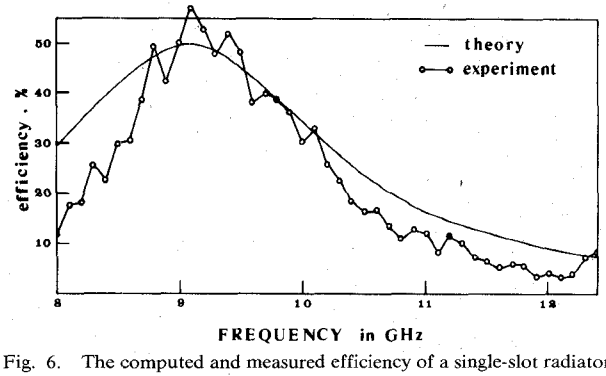

Fig. 6. The computed and measured efficiency of a single-slot radiator.

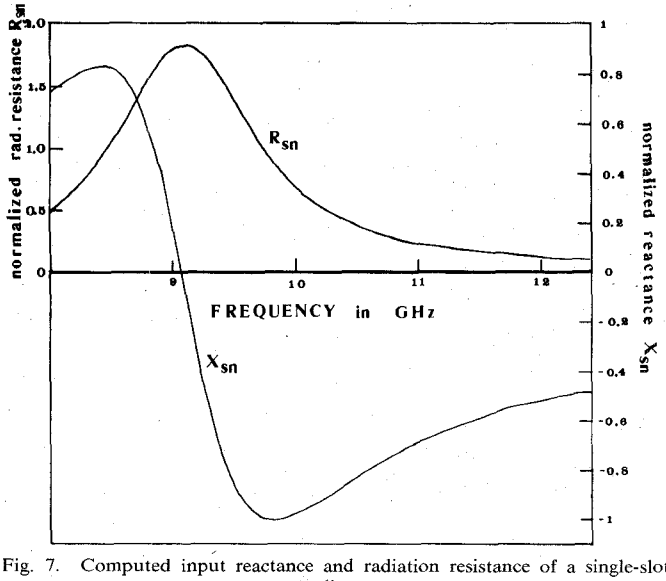

Fig. 7. Computed input reactance and radiation resistance of a single-slot radiator.

9.1 GHz ($d = 0.4532\lambda_{\text{res}}$), which means that the length of the equivalent transmission line is 1.103 times greater than the physical length of the slot. The same phenomenon is observed in the case of a center-fed air slot radiator (see Appendix). The VSWR at resonance is 3.0, and the radiation efficiency is close to 50 percent, as predicted by (34). This means that 50 percent of the incident power is radiated into free space, and the rest is equally divided between the reflected and transmitted waves.

The computed values of the VSWR and radiation efficiency are also shown in Figs. 5 and 6, and there is a fairly good agreement between theory and experiment. The computed active and reactive components of the normalized slot impedance Z_{sn} (28) are plotted in Fig. 7.

Special attention was paid to the possible conversion of the dominant mode to parasitic modes of the empty parallel-plate guide due to the discontinuity caused by the slot. An experimental check was made by closing the gaps between the parallel plates of the guide by metal screens. The screening did not cause any significant changes in the measured values of Γ_0 and P_0, which proved that the parasitic side radiation was below the detection level. Moreover, no detectable side radiation was registered during radiation pattern tests, which showed that its level was at least -40 dB below the slot radiation level. The absence of parasitic side radiation can be explained in the following way. The parallel-plate guides on both sides of the dielectric ($|x| > a/2$, Fig. 1) cannot support any modes with the electric field parallel to the plates because the distance between the plates ($h = 9$ mm) had been chosen less than half the wavelength at the maximum frequency 12.4 GHz. The modes with an electric field perpendicular to the plates are described by the electric field

$$\boldsymbol{E} = \hat{y} E_0 \begin{matrix}\sin\\ \cos\end{matrix}(\gamma_z z)\exp(\pm j\gamma_x x)$$

where $\gamma_z^2 + \gamma_x^2 = k^2$.

Parasitic side radiation would occur if γ_x is real, which means that $\gamma_z^2 < k^2$, and the boundary conditions at $|x| = a/2$ would not be satisfied.

Side radiation in the form of cylindrical waves occurs (and has been observed) only in bended dielectric-loaded parallel-plane guides supporting the dominant H_{10} mode.

Appendix
Evaluation of the Characteristic Impedance and Attenuation Constant of a Center-Fed Slotline

Rigorous expressions for the active and reactive power radiated into a half space by a center-fed narrow slot cut in an infinite conductive sheet (Fig. 8(a)) were obtained by Rhodes [12]

$$P_{\text{rad}} = \frac{|V_0|^2}{2\pi\eta \sin^2(kd/2)} I_p \tag{A1}$$

$$Q_{\text{rad}} = -\frac{|V_0|^2}{2\pi\eta \sin^2(kd/2)} I_q \tag{A2}$$

where

$$\begin{aligned} I_p = {} & [1+\cos(kd)]\,\text{Cin}(kd) - 0.5\,\text{Cin}(2kd)\cos(kd) \\ & + [0.5\,\text{Si}(2kd) - \text{Si}(kd)]\sin(kd) \end{aligned} \tag{A3}$$

$$\begin{aligned} I_q = {} & [1+\cos(kd)]\,\text{Si}(kd) - 0.5\,\text{Si}(2kd)\cos(kd) \\ & + [\text{Cin}(kd) - 0.5\,\text{Cin}(2kd) - 1.5 \\ & + \ln(2w/d)]\sin(kd). \end{aligned} \tag{A4}$$

η and k are given in (4c), and the voltage distribution on the slot is [12]

$$V(x) = V_0 \sin[k(d/2 - |x|)]/\sin(kd/2). \tag{A5}$$

Although the voltage at the ends of the slot is zero [12], the resonance condition of the slot $Q_{\text{rad}} = 0$ is satisfied at $d = 0.4599\lambda_{\text{res}}$ (for $d/w = 12.0$).

A lossy transmission line with the same voltage distribution (Fig. 8(b)) is equivalent to the radiating slot [9]. The length b of the line is half the slot resonance wavelength. The active and

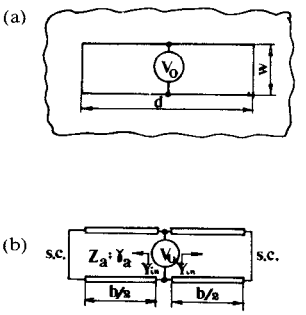

Fig. 8. Center-fed air slot dipole and its equivalent circuit.

reactive power delivered to the input of the line are

$$P_{\text{in}} = \frac{|V_0|^2}{Z_a} \frac{\tanh(\alpha_a b/2)}{\sin^2(kb/2) + \tanh^2(\alpha_a b/2)\cos^2(kb/2)} \tag{A6}$$

$$Q_{\text{in}} = \frac{|V_0|^2}{Z_a} \frac{\text{cotan}(kb/2)}{\cosh^2(\alpha_a b/2) + \text{cotan}^2(kb/2)\sinh^2(\alpha_a b/2)} \tag{A7}$$

where α_a and Z_a are the attenuation constant and the characteristic impedance of the line.

Since the length of the slot is less than half the resonant wavelength, the length of the equivalent transmission line is larger than the physical length of the slot, i.e., $b = 1.0871d$.

Explicit expressions for α_a and Z_a are obtained by equating P_{rad} with P_{in}, and Q_{rad} with Q_{in}

$$\alpha_a = \frac{1}{b}\sinh^{-1}\frac{I_p}{I_q}\sin(kb) \tag{A8}$$

$$Z_a = \frac{2\pi\eta}{I_p} \frac{\sin^2(kd/2)\tanh(\alpha_a b/2)}{\sin^2(kb/2) + \tanh(\alpha_a b/2)\cos^2(kb/2)}. \tag{A9}$$

From (A9), it follows that $Z_a \approx 430\ \Omega$ with a very slight frequency dependence.

Finally, consider an empty rectangular guide, supporting the dominant mode, with a symmetrical transverse slot in the broad wall. At the quasi-resonant frequency of the slot $d = \lambda/2$, the equivalent normalized resistance of the slot is found from (28) after the substitutions of $h = b$, $v = 0.25\pi\lambda/a$, $u = \alpha_a d/2 + j\pi/2$, and

$$\beta_g/k = \lambda/\lambda_g \quad \tanh(u) = \frac{1}{\tanh(\alpha_a d/2)}.$$

From (28b) and (28c), it follows

$$\begin{aligned} Q_1 = {} & -2u^2 \frac{\cos^2 v}{\tanh(\alpha_a d/2)} - uv\sin(2v) \\ & + u(u^2+v^2)[1+\text{sinc}(2v)] \end{aligned}$$

$$Q_2 = (u^2+v^2)^2.$$

Since $\alpha_a d/2 \ll \pi/2$, the following approximations are assumed:

$$u \approx j\pi/2 \quad Q_1 \approx \frac{\pi^2}{2}\frac{\cos^2 v}{\tanh(\alpha_a d/2)} \quad Q_2 = \left(\frac{\pi}{2}\right)^4\left(\frac{\lambda}{\lambda_g}\right)^4$$

and $\text{sinc}(\beta_g w/2) \approx 1$.

The substitution of these approximate expressions into (28a) leads to

$$Z_{sn} = \frac{Z_a}{\tanh(\alpha_a d/2)} \frac{\lambda^2}{ab\eta\pi^2}\left(\frac{\lambda_g}{\lambda}\right)^3 \cos^2\left(\frac{\pi\lambda}{4a}\right). \tag{A10}$$

From (A9), it follows that at $kd = \pi$ ($I_p \approx 1.23$)

$$\frac{Z_a}{\tanh(\alpha_a d/2)} \approx \frac{2\pi\eta}{I_p}. \quad \text{(A11)}$$

After the substitution of (A11) into (A10), the normalized impedance of the slot is

$$Z_{sn} = \frac{2}{1.23\pi}\frac{\lambda^2}{ab}\left(\frac{\lambda_g}{\lambda}\right)^3 \cos^2\left(\frac{\pi\lambda}{4a}\right)$$

which is the classical Stevenson formula [6], [7].

ACKNOWLEDGMENT

The authors would like to acknowledge the contribution of J. Nissim, who performed the computer calculations.

REFERENCES

[1] L. Lewin and T. Ruehle, "A note on the complex Poynting vector and on the fractional current on the upper surface of a microstrip line," *IEEE Trans. Antennas Propagat.*, vol. AP-29, pp. 144–147, Jan. 1981.

[2] F. J. Tisher, "A waveguide structure with low losses," *Arch. Elek Übertragung.*, pp. 592–596, Dec. 1953.

[3] F. J. Tisher, "The *H*-guide, a waveguide for microwaves," in *1956 IRE Convention Rec.*, pt. 5, pp. 44–47.

[4] M. Cohn, "Propagation in a dielectric-loaded parallel plane waveguide," *IRE Trans. Microwave Theory Tech.*, vol. MTT-7, pp. 202–208, Apr. 1959.

[5] R. F. B. Conlon and F. A. Benson, "Propagation and attenuation in the double-strip *H*-guide," *Proc. Inst. Elec. Eng.*, vol. 113, pp. 1311–1320, Aug. 1966.

[6] A. F. Stevenson, "Theory of slots in rectangular waveguides," *J. Appl. Phys.*, vol. 19, pp. 24–38, Jan. 1948.

[7] S. Silver, Ed., *Microwave Antenna Theory and Design* (MIT Rad. Lab. Ser., vol. 12). New York: McGraw-Hill, 1949, pp. 287–291.

[8] M. Kisliuk, "The conformal microstrip slot antenna," in *1983 IEEE Int. Symp. Antennas and Propagat.* (Houston, TX), vol. 1, pp. 166–169.

[9] M. Kisliuk, "The voltage distribution on waveguide fed slot and slit antennas," in *IEEE Benjamin Franklin Symp. on Advances in Antenna and Microwave Technology Dig.*, (Philadelphia, PA), 1983, pp. 13–15.

[10] S. Cohn, "Slot line on a dielectric substrate," *IEEE Trans. Microwave Theory Tech.*, vol. MTT-17, pp. 768–778, Oct. 1969.

[11] R. C. Hansen, *Microwave Scanning Antennas*, vol. 3. New York and London: Academic Press, 1964.

[12] D. R. Rhodes, "On the stored energy of planar apertures," *IEEE Trans. Antennas Propagat.*, vol. AP-14, pp. 676–683, Nov. 1966.

Large-Signal Equivalent-Circuit Model of a GaAs Dual-Gate MESFET Mixer

ROBERT E. MILES, MEMBER, IEEE, AND
MICHAEL J. HOWES, SENIOR MEMBER, IEEE

***Abstract*—A large-signal equivalent-circuit model of a GaAs dual-gate MESFET mixer containing twelve elements, of which eight are voltage-dependent, is solved in the time domain for local oscillator and signal frequencies of 9.5 GHz and 10.0 GHz, respectively. The results give the variation of conversion gain with local oscillator and signal power levels and are in good agreement with measured values. The model is formulated in such a way that material/device/circuit interactions can be studied, yielding information on the preferred device structures and biasing conditions.**

Manuscript received September 12, 1984; revised January 4, 1985.

R. E. Miles is with the Microelectronics Centre of the University of Bradford, Bradford BD7 1HR, England.

M. J. Howes is with the Department of Electrical and Electronic Engineering, University of Leeds, Leeds LS2 9JT, England.

I. INTRODUCTION

As GaAs microwave integrated circuits emerge as viable systems, one of the most important applications is predicted [1] to be in direct broadcasting by satellite (DBS) television with worldwide market possibilities. An essential requirement for this technology is an integrated-circuit 'front-end' to be mounted on the receiving dish. The dual-gate MESFET mixer is probably the best solution to the down conversion in this system because it has the advantages of a reasonable noise figure and conversion gain (as opposed to a loss for Schottky diodes), and the inherent separation of signal and local oscillator inputs results in circuit simplification with consequent economies in chip surface area.

With this application in mind, a large-signal equivalent-circuit model of a dual-gate MESFET in a mixer configuration is presented. Using dc characteristics and analytical expressions for the voltage dependence of the capacitance of a Schottky barrier, the model is solved in the time domain over one period of the IF, and the resulting output is Fourier analyzed to determine the frequency components produced. The advantages of this method of solution are that the mixing process can be well understood and illustrated under all conditions of bias, and also the relationship between the material parameters and the circuit performance can be elucidated.

II. DERIVATION OF THE MODEL

A. Low-Frequency Model

At low frequencies, the effects of reactive components can be ignored and the mixing properties of the device derived using $I_{DS}-V_{DS}$ characteristics. In common with other published work [2], [3], the dual-gate FET is modeled here as two single-gate FET's in cascode with the dain of FET 1 connected to the source of FET 2. The signal (RF) is applied to the gate of FET 1 and the local oscillator (LO) to that of FET 2. This is illustrated schematically in Fig. 1, which also shows the important voltages used in the calculations. In order to obtain a solution to this circuit, an analytical expression for the output characteristics of each component FET is required. For this work, the expression used is based on that suggested by Gopinath and Rankin [4], i.e.,

$$I_{DS} = \left(1-\frac{V_{DS}}{V_p}\right)^2\left(I_{DSS}+\frac{V_{DS}}{R_{DO}}\right)$$

for $V_{DS} > V_{TAN}$, i.e., the saturation region (1a)

and

$$I_{DS} = \left(1-\frac{V_{GS}}{V_p}\right)^2\left[I_{DSS}+\frac{V_{DS}}{R_{DO}}-I_{DSS}\left(\frac{V_{TAN}-V_{DS}}{V_{TAN}}\right)^3\right]$$

for $V_{DS} < V_{TAN}$. (1b)

In these equations, V_p is the gate pinchoff voltage, I_{DSS} the drain–source saturation current, and R_{DO} the output resistance.

V_{TAN} defines the boundary between resistive and saturation behavior where

$$V_{TAN} = V_{OO}\left[1+\left(1+\frac{2R_{DO}I_{DSS}}{V_{OO}}\right)^{1/2}\right]$$

with

$$V_{OO} = \frac{\left(1-\frac{V_{GS}}{V_p}\right)^2 V_{DT}^2}{2(I_{DSS}R_{DO}+V_{DT})} \text{ and } V_{DT} = 2.25 \text{ V}.$$

0018-9480/85/0500-0433$01.00 ©1985 IEEE